Supplementary Information (SI) for Journal of Materials Chemistry C.

Supporting Information

Switching the heavy-atom effect in blue thermally activated delayed fluorescence emitters

*Jan Szumilas, Chi Hyun Ryoo, Michał Mońka, Piotr Bojarski, Soo Young Park,**

*Illia E. Serdiuk**

Contents

Additional PL spectra

A)

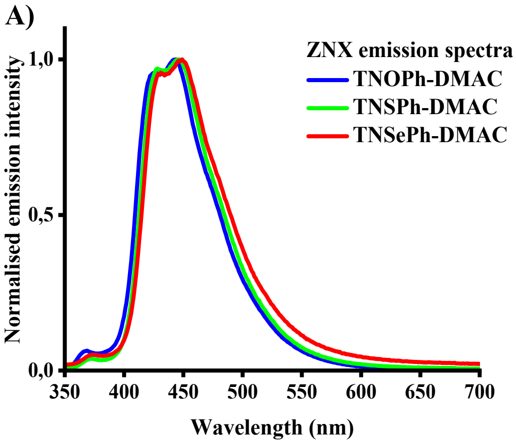

B)

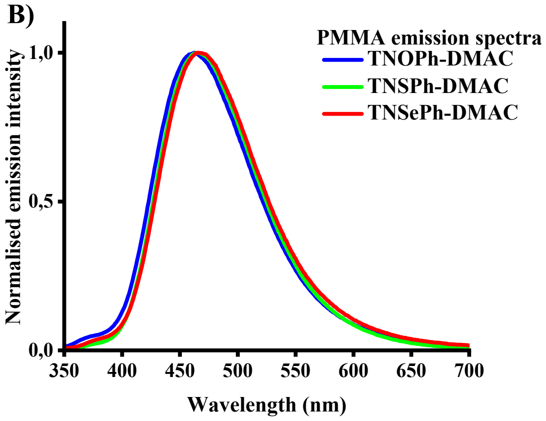

C)

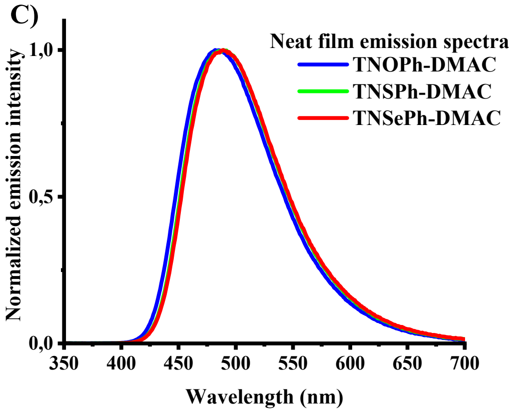

D)

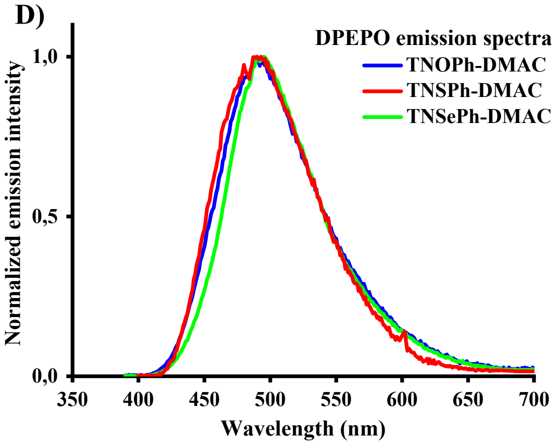

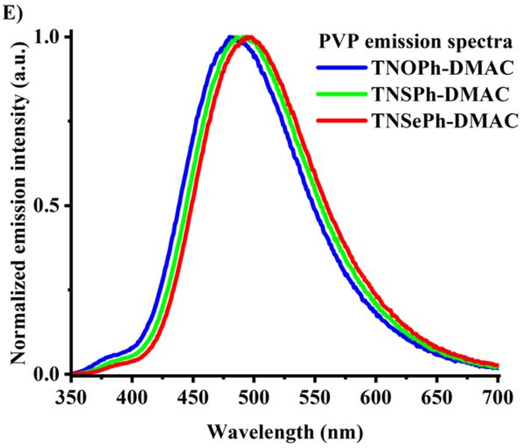

Figure S1. Steady state emission spectra in ZNX (A) and PMMA (B), neat (C), DPEPO (D), and PVP (E) films.

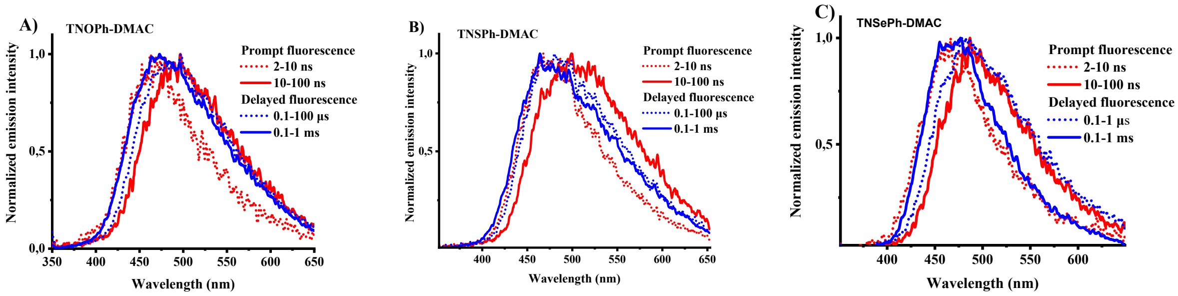

Figure S2. Time-resolved emission spectra of **TNOPh-DMAC** (A), **TNSPh-DMAC** (B), and **TNSePh-DMAC** (C) in doped PMMA films.

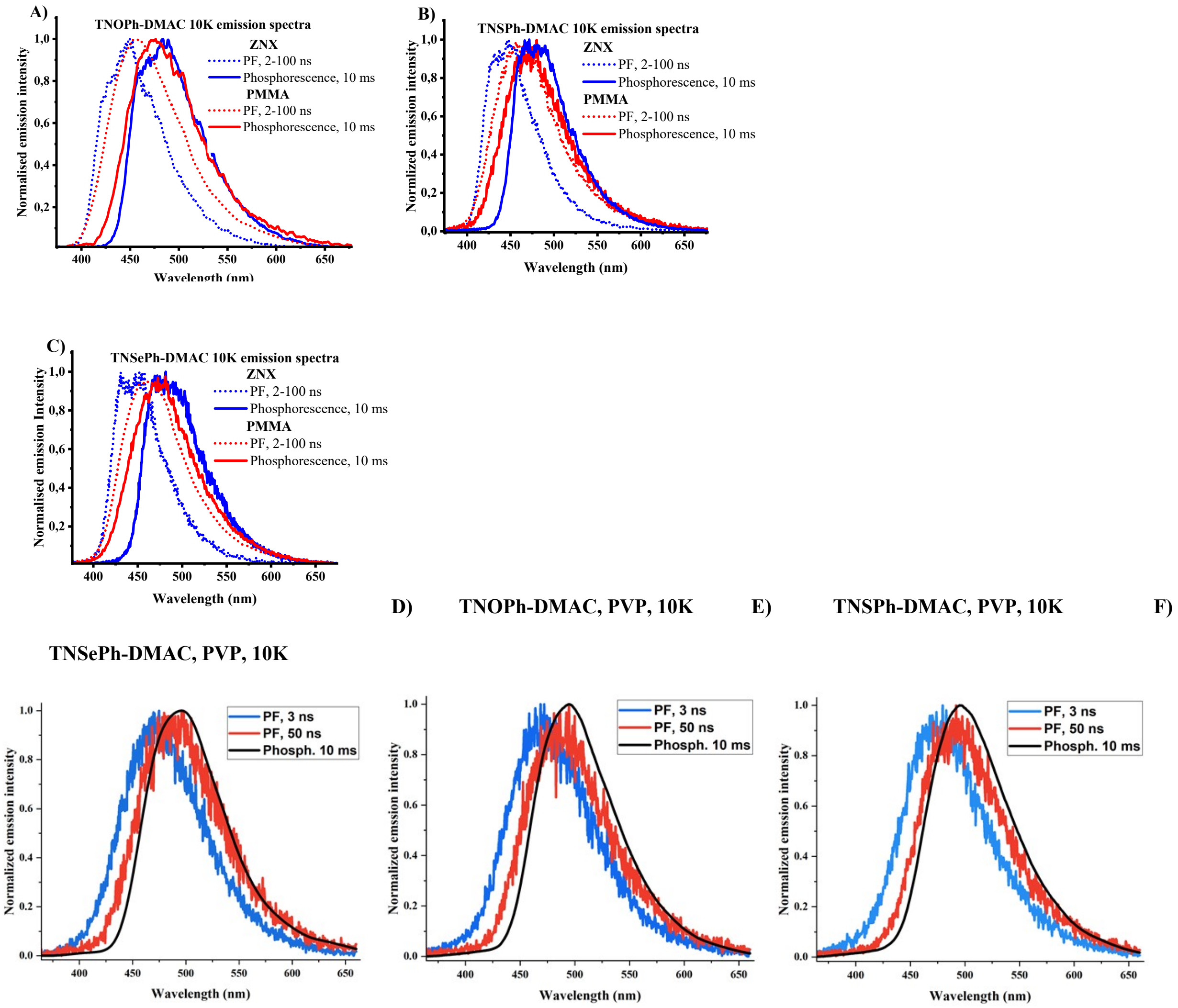

Figure S3. Time-resolved emission spectra for the investigated compounds in various media at 10K: **TNOPh-DMAC** (A, D), **TNSPh-DMAC** (B, E) and **TNSePh-DMAC** (C, F).

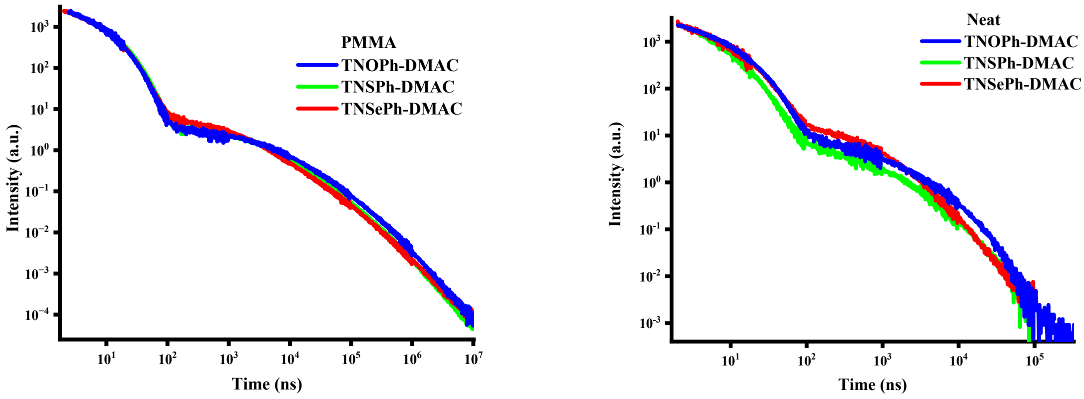

Figure S4. Emission decays in various media at room temperature (RT) under vacuum in PMMA and neat films.

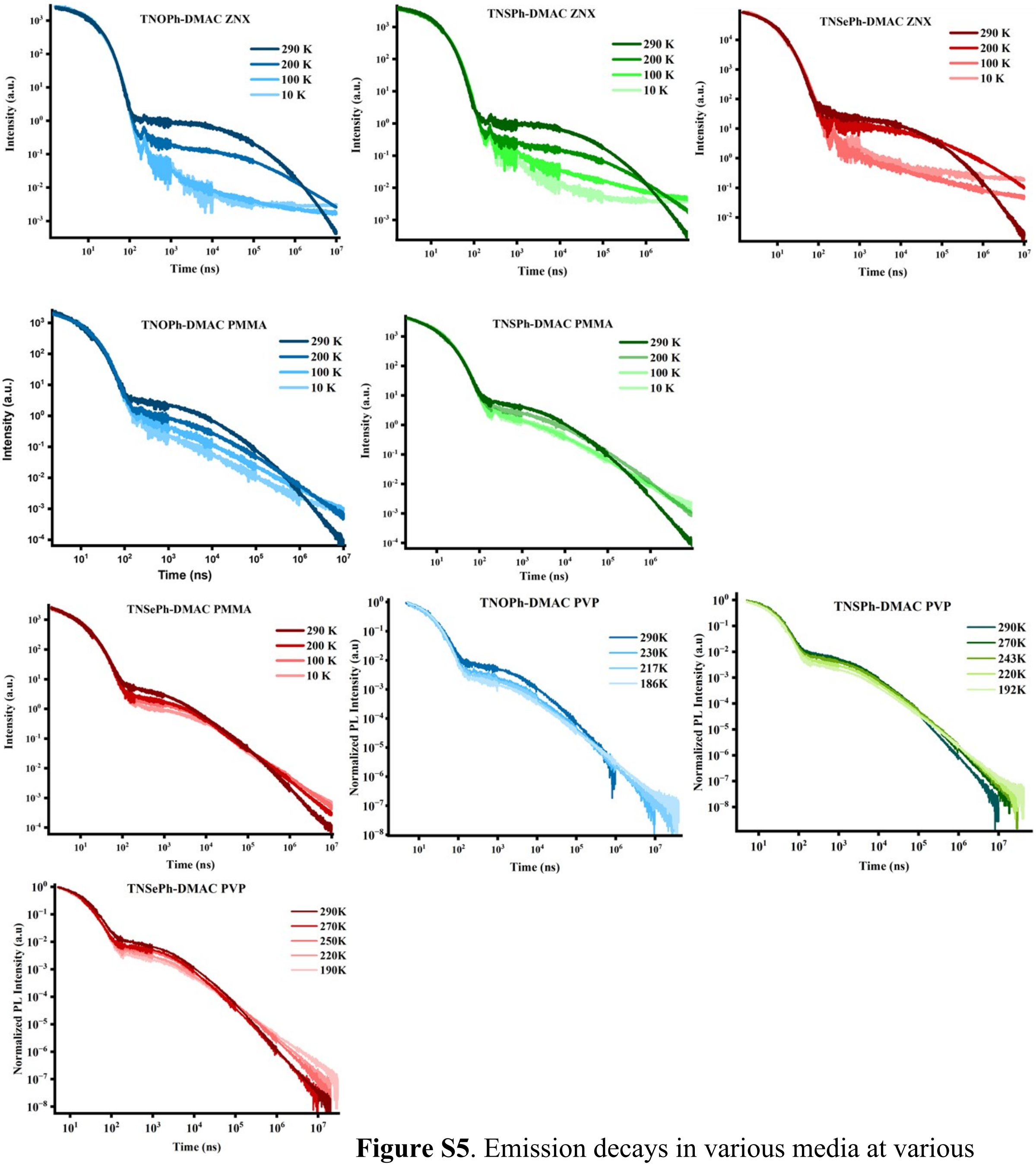

Figure S5. Emission decays in various media at various temperatures.

Quantum chemical calculations

Rotational isomerism

DFT calculations revealed two distinct local minima for all investigated compounds, differentiated by the dihedral angle between the phenyl group and chalcogen-*s*-triazine fragment. As such, geometry optimization and orbital calculations have been performed for both group A (phenyl ring oriented towards donor fragment) and B (phenyl ring oriented away from the donor fragment). In optimal structures, such an dihedral angle α equals 59° (A) and 55° (B) in TNOPh-DMAC, and 90° in both configurations of TNSPh-DMAC and TNSePh-DMAC

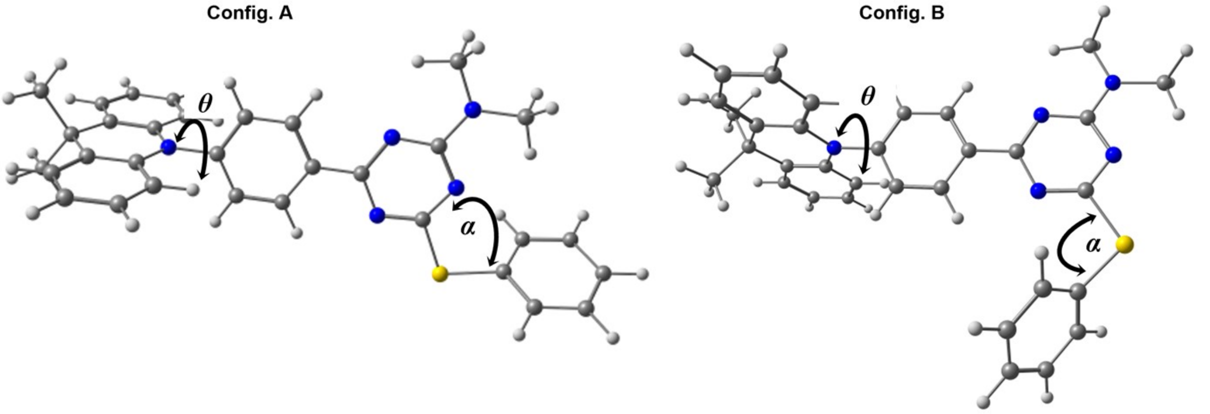

The influence of the dihedral angle θ between the acceptor and donor fragments has been taken into account to estimate the influence of the ^{3}CT-^{1}CT transitions. As follows from the previous studies,[S1] the electronic features of the rotational isomer with $\theta = 82^{o}$ reflects well the statistical sum of such θ rotamers. The parameters of the ^{3}CT-^{1}CT transition is presented thus for respective geometries with a fixed $\theta = 82^{o}$.

Molecular orbitals and SOC constants

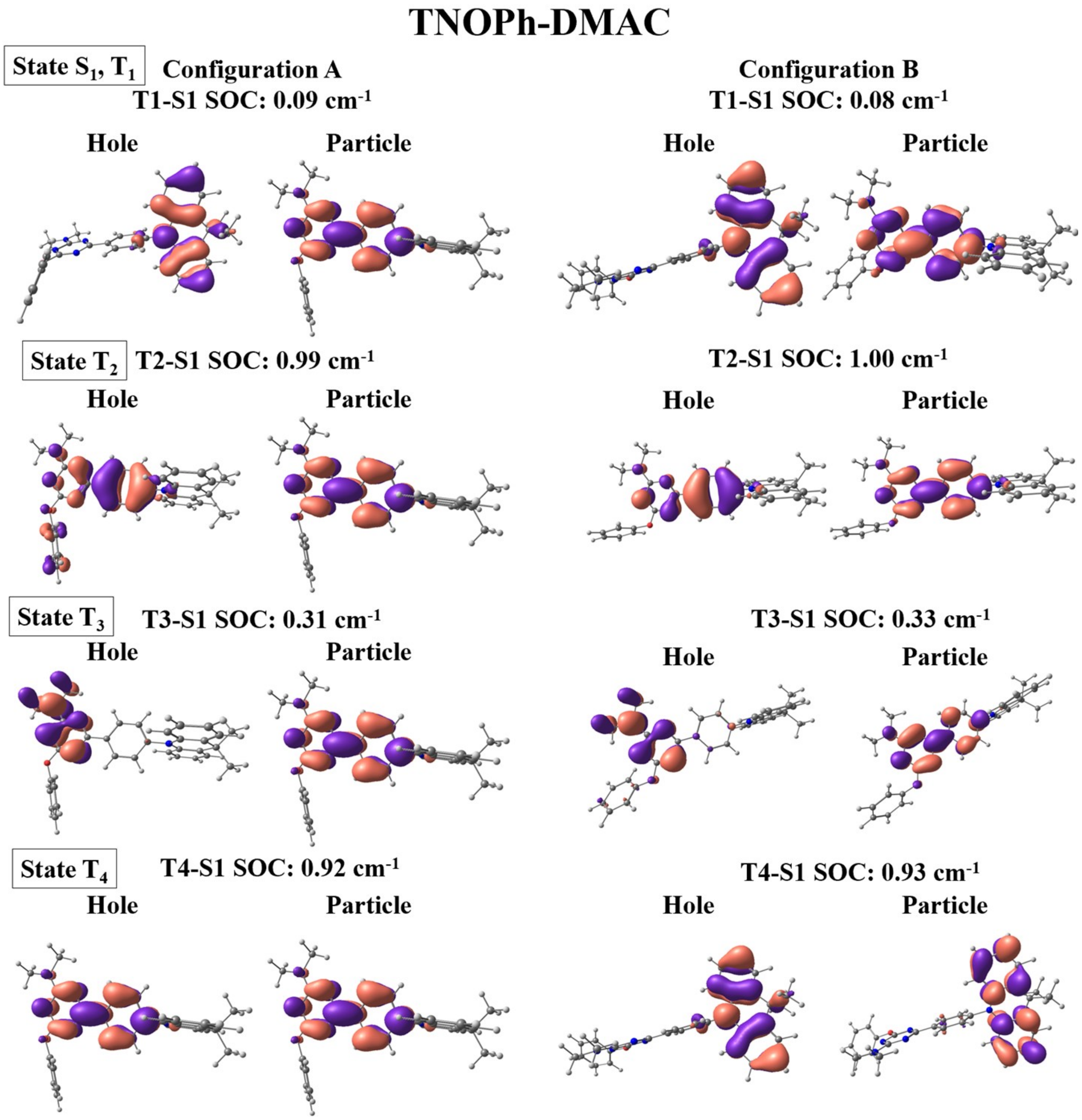

Figure S6. Natural transition orbitals and SOC constants of selected low-energy transitions in **TNOPh-DMAC**.

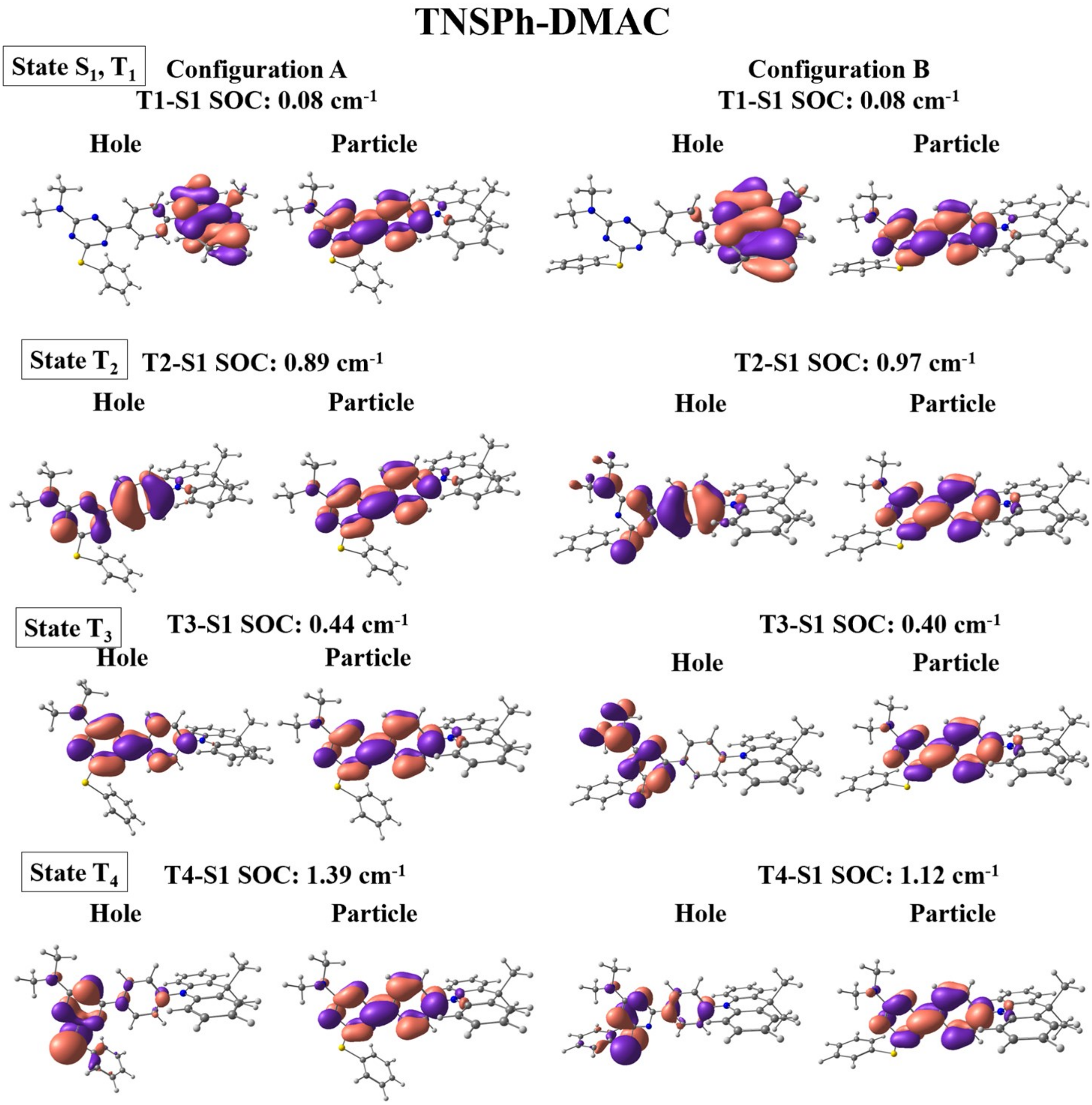

Figure S7. Natural transition orbitals and SOC constants of selected low-energy transitions in **TNSPh-DMAC**.

TNSePh-DMAC

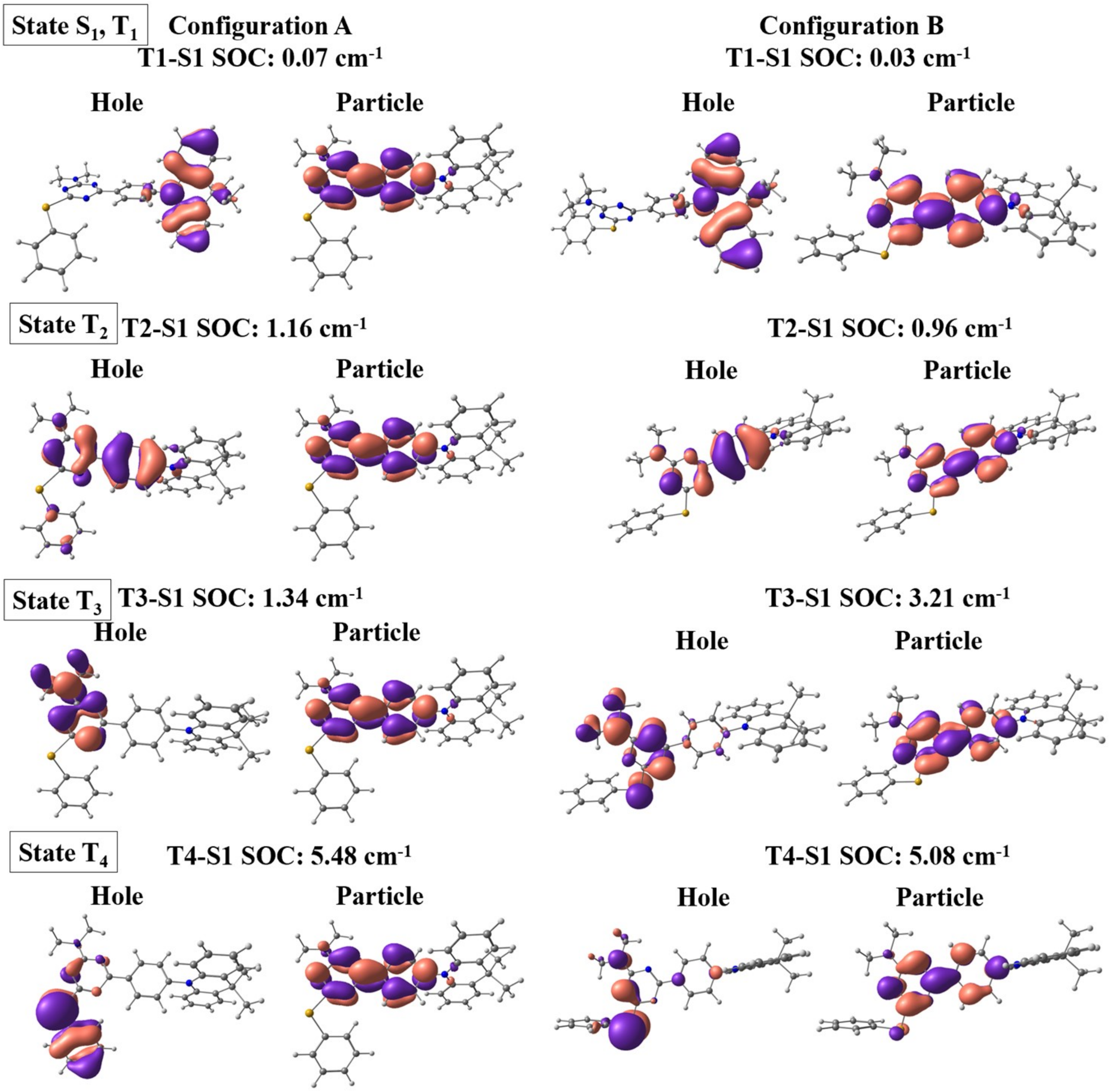

Figure S8. Natural transition orbitals and SOC constants of selected low-energy transitions in **TNSePh-DMAC**.

Table S1. TD-DFT predicted SOC constants for the $T_2(^3LE)$-S_0 and $T_1(^3CT)$-S_0 transitions.

Compound	**TNOPh-DMAC**		**TNSPh-DMAC**		**TNSePh-DMAC**	
State	T_1 (^{3}CT)	T_2 (^{3}LE)	T_1 (^{3}CT)	T_2 (^{3}LE)	T_1 (^{3}CT)	T_2 (^{3}LE)
SOC [cm^{-1}]	2.1	0.1	2.0	0.1	1.4	0.1

Table S2. Selected electronic parameters for A and B configurations.

Compound	**Config.**	**HOMO [eV]**	**LUMO [eV]**	**^{3}LE-^{1}CT**			**^{3}CT-^{1}CT**		
				λ [eV]	**ΔE [eV]**	**SOC [10^{-4} eV]**	**λ [eV]**	**ΔE [eV]**	**SOC [10^{-6} eV]**
TNOPh-DMAC	A	-4.97	-1.96	0.25	0.595	1.2	0.025	0.032	11.2
TNSPh-DMAC	A	-4.97	-1.97	0.23	0.571	1.1	0.021	0.027	9.9
TNSePh-DMAC	A	-4.97	-1.96	0.27	0.452	6.8	0.024	0.029	8.8
TNOPh-DMAC	B	-5.01	-2.00	0.26	0.608	1.2	0.023	0.030	10.0
TNSPh-DMAC	B	-5.00	-2.00	0.24	0.585	1.2	0.021	0.028	9.9
TNSePh-DMAC	B	-4.99	-1.98	0.24	0.577	1.2	0.017	0.024	4.1

Effect of concentration of emitter

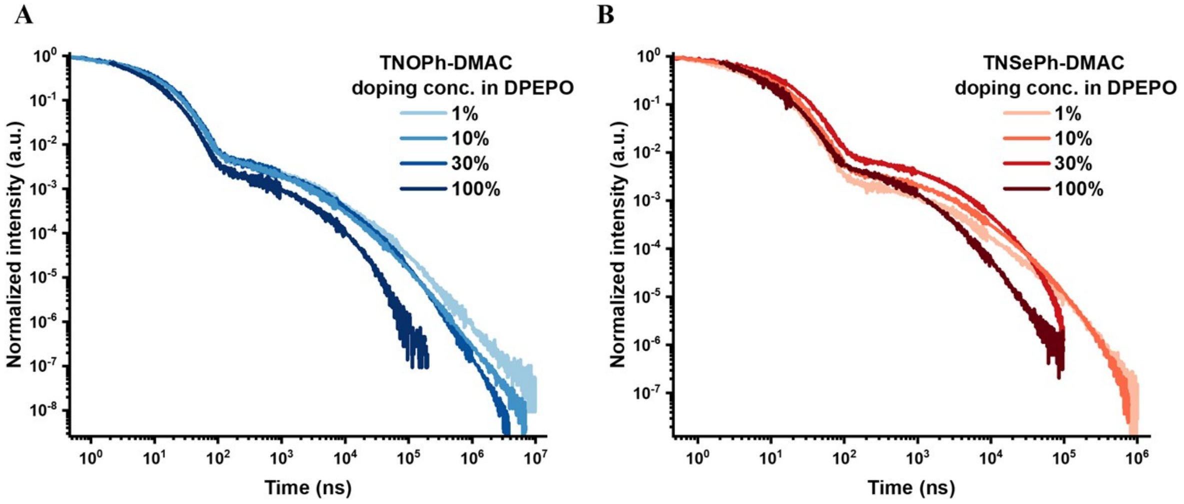

Figure S9. PL decay curves at different concentration of emitter in DPEPO host: **A - TNSPh-DMAC** and **B - TNSePh-DMAC**

Table S3. Summary of photophysical parameters in neat films and **TNSPh-DMAC** doped DPEPO film.

Compound	Conc. *w/w*	$\mathrm{PL_{max}}$ [nm]	τ_{PF} [ns]	τ_{DF} [μs]	PLQY [%]	k_{r} [10^7, $\mathrm{s^{-1}}$]	k_{ISC} [10^7, $\mathrm{s^{-1}}$]	k_{nr} [10^7, $\mathrm{s^{-1}}$]	k_{rISC} [10^4, $\mathrm{s^{-1}}$]
TNOPh-DMAC	100% (neat)	480	12.5	6.6	59	2.8	3.2	2.0	25
TNSPh-DMAC	100% (neat)	478	8.7	5.7	52	2.3	3.5	2.3	25
TNSePh-DMAC	100% (neat)	483	12.8	3.8	49	2.8	2.1	2.9	36
TNSPh-DMAC	10%	494	15.1	58	67	1.7	4.1	0.8	4.5

^{1}H NMR spectra in CDCl$_3$

TNOPh-DMAC

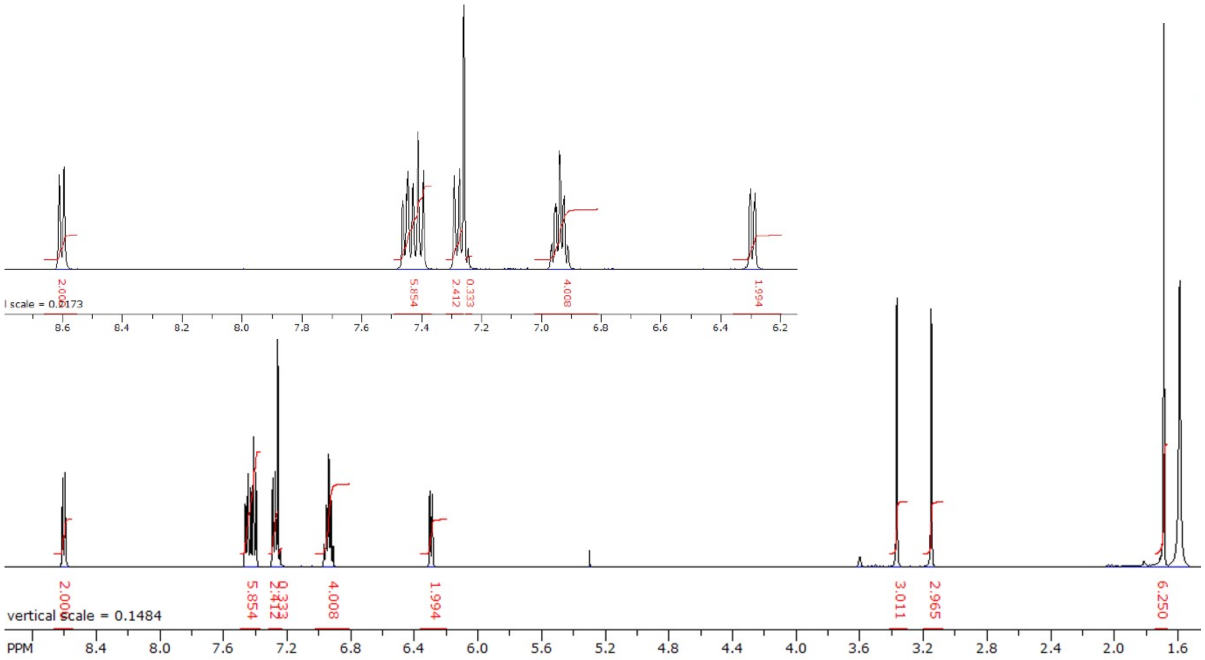

TNSPh-DMAC

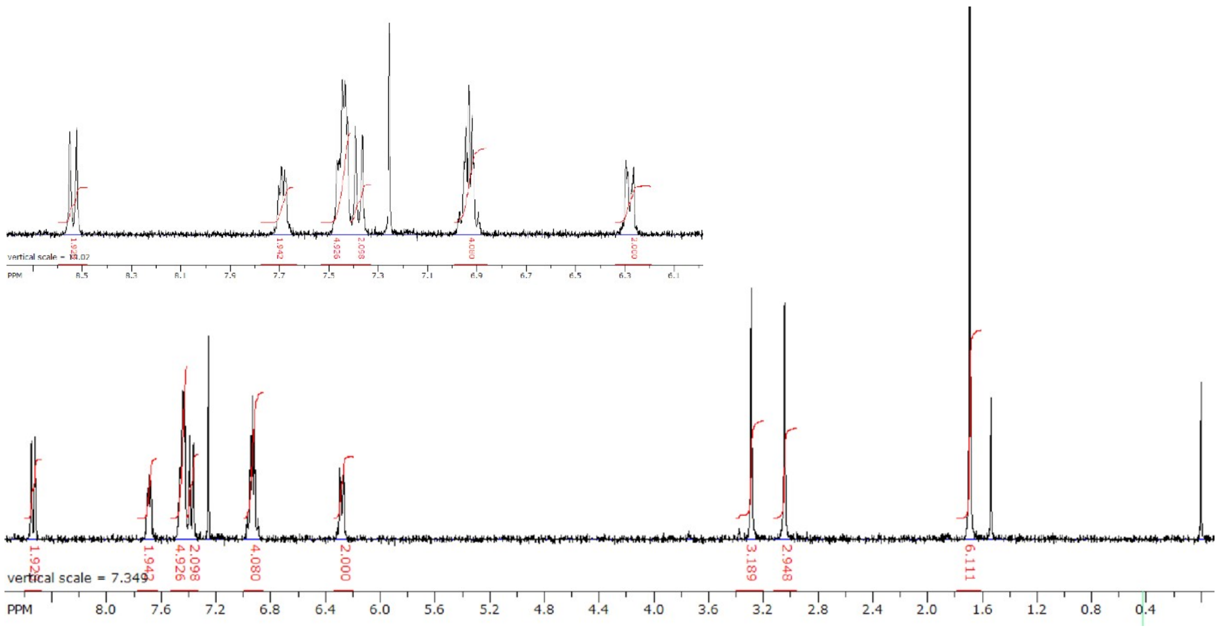

TNSePh-DMAC

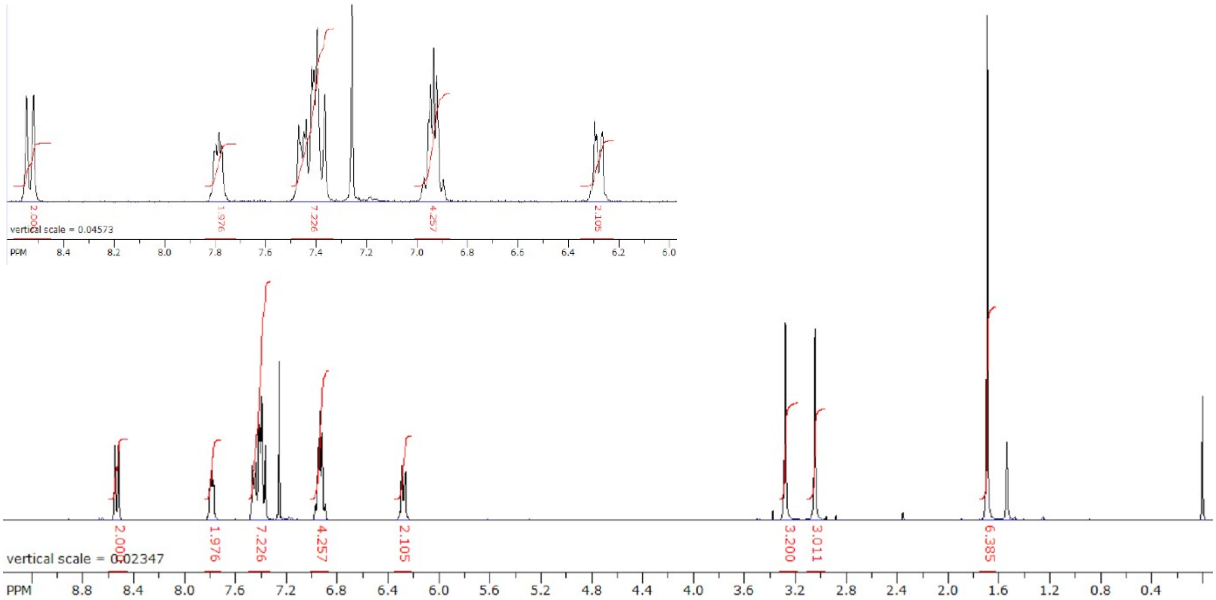
2.000
1.976
7.226
4.257
2.105
vertical scale = 0.04573
PPM
8.4
8.2
8.0
7.8
7.6
7.4
7.2
7.0
6.8
6.6
6.4
6.2
6.0
2.000
1.976
7.226
4.257
2.105
3.200
3.011
6.385
vertical scale = 0.02347
PPM
8.8
8.4
8.0
7.6
7.2
6.8
6.4
6.0
5.6
5.2
4.8
4.4
4.0
3.6
3.2
2.8
2.4
2.0
1.6
1.2
0.8
0.4

^{13}C NMR spectra in CDCl$_3$

TNOPh-DMAC

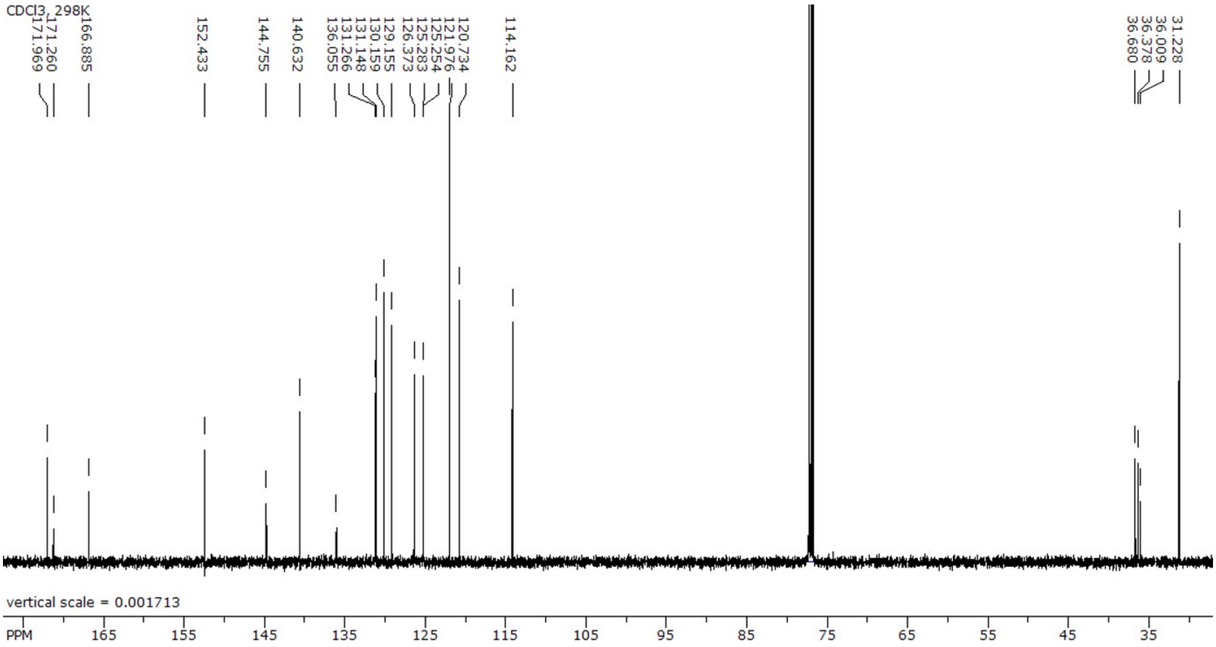

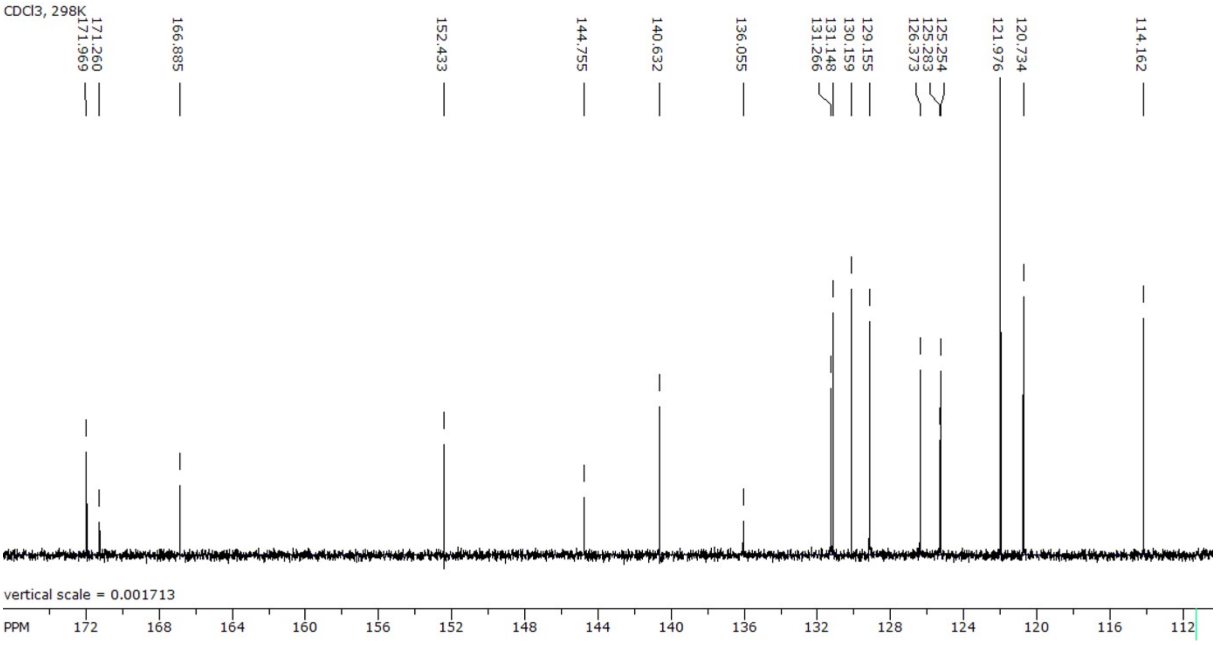

TNSPh-DMAC

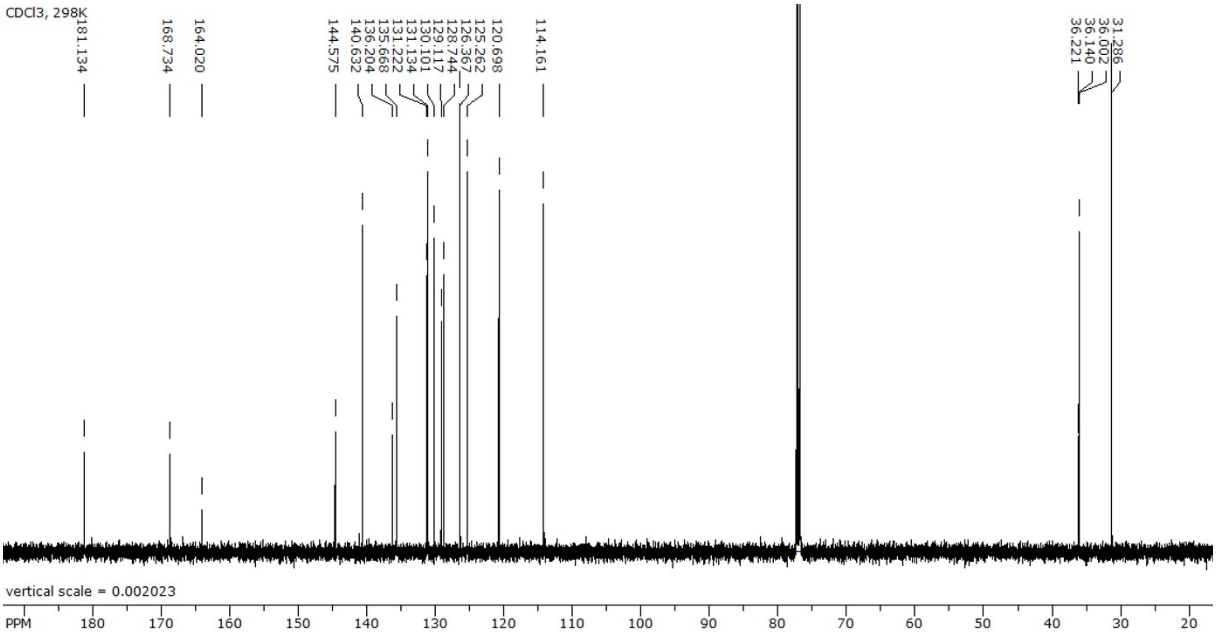
CDCl3, 298K
181.134
168.734
164.020
144.575
140.632
136.204
135.668
131.222
131.134
130.101
129.117
128.744
126.367
125.262
120.698
114.161
31.286
36.002
36.140
36.221
vertical scale = 0.002023
PPM
180
170
160
150
140
130
120
110
100
90
80
70
60
50
40
30
20

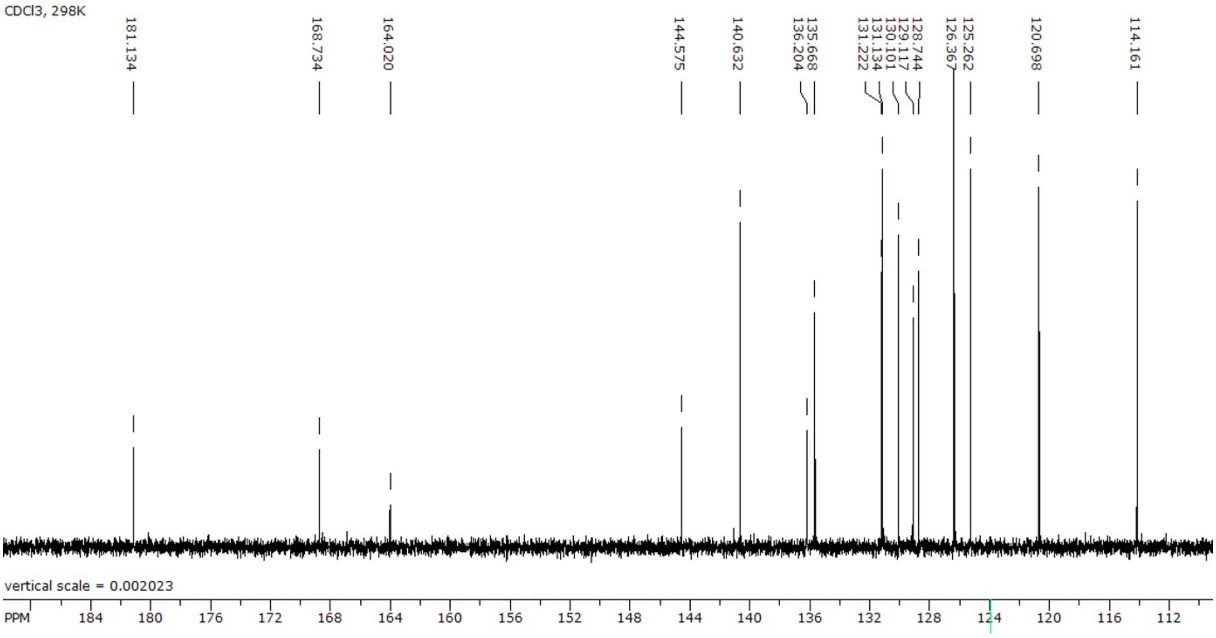
CDCl3, 298K
181.134
168.734
164.020
144.575
140.632
135.668
136.204
131.134
131.222
130.101
129.117
128.744
126.367
125.262
120.698
114.161
vertical scale = 0.002023
PPM
184
180
176
172
168
164
160
156
152
148
144
140
136
132
128
124
120
116
112

TNSePh-DMAC

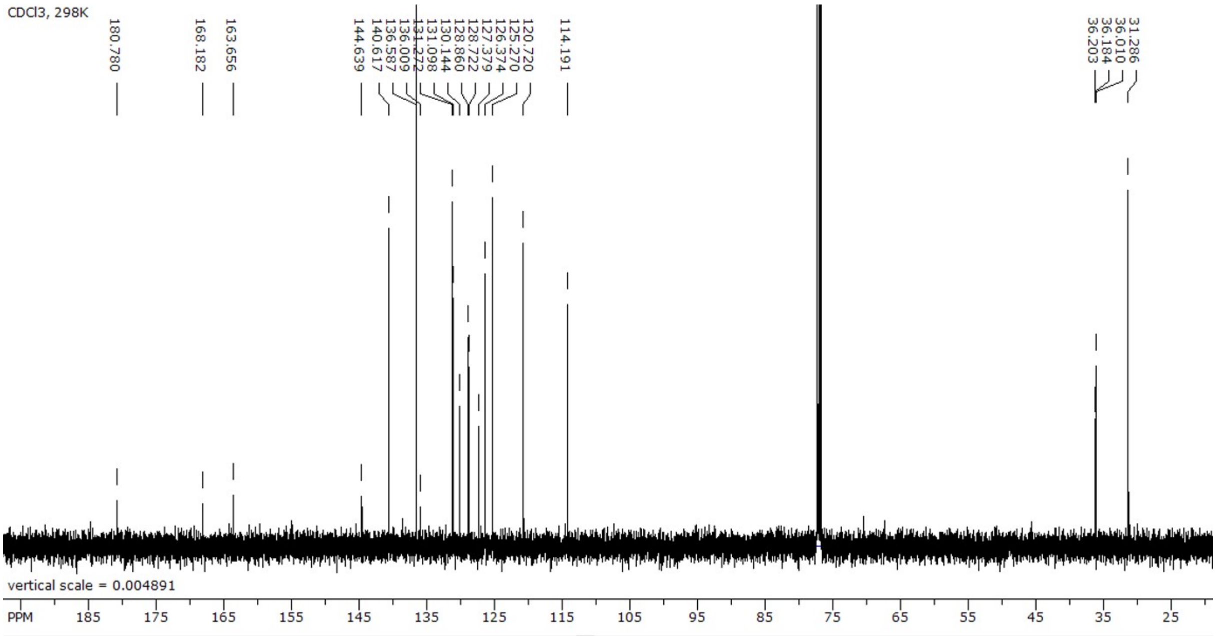

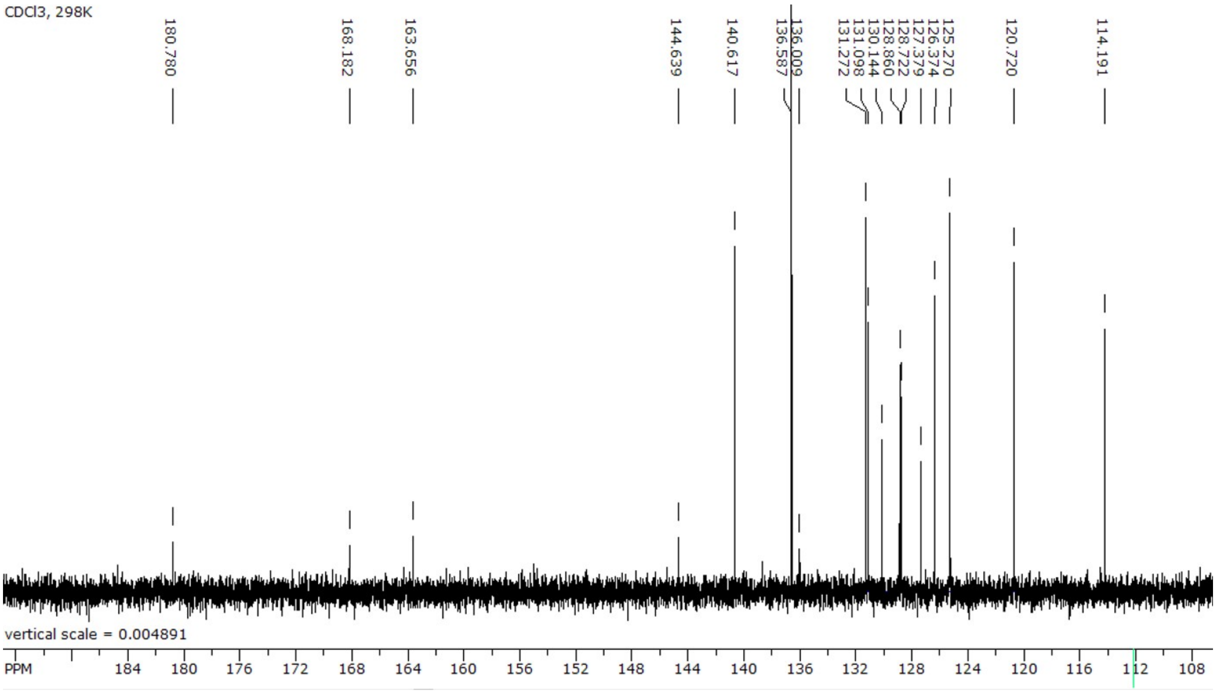

References

[S1] Ryoo, C. H.; Han, J.; Yang, J.-H.; Yang, K.; Cho, I.; Jung, S.; Kim, S.; Jeong, H.; Lee, C.; Kwon, J. E.; Serdiuk, I. E.; Park, S. Y. Systematic Substituent Control in Blue Thermally Activated Delayed Fluorescence (TADF) Emitters: Unraveling the Role of Direct Intersystem Crossing between the Same Charge-Transfer States. *Adv. Optical Mater.* 2022, *10*, No. 2201622.